THE JOURNAL OF BIOLOGICAL CHEMISTRY VOL. 282, NO. 11, pp. 8356–8367, March 16, 2007
Printed in the U.S.A.

Mutational Study of Heparan Sulfate 2-*O*-Sulfotransferase and Chondroitin Sulfate 2-*O*-Sulfotransferase*

Received for publication, August 22, 2006, and in revised form, January 8, 2007 Published, JBC Papers in Press, January 15, 2007, DOI 10.1074/jbc.M608062200

Ding Xu[‡1], **Danyin Song**[‡], **Lars C. Pedersen**[§], **and Jian Liu**[‡2]

From the [‡]*Division of Medicinal Chemistry and Natural Products, School of Pharmacy, University of North Carolina, Chapel Hill, North Carolina 27599 and* [§]*Laboratory of Structural Biology, NIEHS, National Institutes of Health, Research Triangle Park, North Carolina 27709*

Heparan sulfate (HS) and chondroitin sulfate (CS) are highly sulfated polysaccharides with a wide range of biological functions. Heparan sulfate 2-*O*-sulfotransferase (HS-2OST) transfers the sulfo group from 3′-phosphoadenosine 5′-phosphosulfate (PAPS) to the 2-OH position of the hexauronic acid that is adjacent to *N*-sulfated glucosamine, whereas chondroitin sulfate 2-*O*-sulfotransferase (CS-2OST) transfers the sulfo group to the hexauronic acid that is adjacent to *N*-acetylated galactosamine. Here we report a systematic mutagenesis study of HS-2OST and CS-2OST based on their structural homology to estrogen sulfotransferase and HS 3-*O*-sulfotransferase isoform 3 (3-OST3), for which crystal structures exist. We have identified six residues possibly involved in binding to PAPS. HS-2OST carrying mutations of these residues lacks sulfotransferase activity and the ability to bind 3′-phosphoadenosine 5′-phosphate, a PAPS analogue, as determined by isothermal titration calorimetry. Similar residues involved in binding to PAPS were also identified in CS-2OST. Additional residues that participate in carbohydrate substrate binding were also identified in both enzymes. Mutations at these residues led to the loss of sulfotransferase activity but maintained the ability to bind to phosphoadenosine 5′-phosphate. The catalytic function of HS-2OST appears to involve two histidine residues (His^{140} and His^{142}), whereas only one histidine (His^{168}) of CS 2-OST is likely to be critical. This unique feature of HS 2-OST catalytic residues directed us to characterize the *Drosophila* heparan sulfate 2-*O*-sulfotransferase. The results from this study provide insight into the differences and similarities various residues play in the biological roles of the HS-2OST and CS-2OST enzymes.

Glycosaminoglycan is a ubiquitous macromolecule existing in large quantities on the cell surface and in the extracellular matrix. Glycosaminoglycan consists of heparan sulfate (HS)[3] and chondroitin sulfate (CS) polysaccharides with different disaccharide repeating units. Growing evidence suggests that glycosaminoglycans have diverse roles in regulating embryonic development, neuron development, blood coagulation, immune response, carcinogenesis, virus infection, wound repair, etc., mainly through the HS or CS chains with specific structures (1, 2). The diverse structures of HS and CS are synthesized by complex biosynthetic pathways, which take place in the Golgi apparatus. The HS backbone is synthesized as a copolymer of GlcUA and *N*-acetylated glucosamine (GlcNAc) by HS copolymerase EXT1 and EXT2, followed by various modifications. These modifications include *N*-deacetylation and *N*-sulfation of GlcNAc, C5 epimerization of glucuronic acid to form IdoUA residues, 2-*O*-sulfation of or GlcUA residues, and 6-*O*-sulfation and 3-*O*-sulfation of glucosamine residues (3, 4). The CS backbone is synthesized as a copolymer of GlcUA and *N*-acetylated galactosamine (GalNAc) by the chondroitin synthase and chondroitin polymerizing factor, cooperatively (5). The modifications of CS chain include 4-*O*-sulfation or 6-*O*-sulfation on GalNAc, C5 epimerization of GlcUA to IdoUA, and 2-*O*-sulfation on GlcUA or IdoUA (3, 6).

The biological significance of 2-*O*-sulfated IdoUA in HS, by HS-2OST, has been demonstrated by *in vitro* and *in vivo* studies. The 2-*O*-sulfation of IdoUA by HS-2OST is necessary for the binding to many members of the fibroblast growth factor family, essential for the initiation of fibroblast growth factor-mediated signal transduction pathways (7, 8). The HS-2OST knock-out mice show renal agenesis and die in the neonatal period, and they have over-mineralized skeletons and show retardation of eye development (9). In *Caenorhabditis elegans*, HS-2OST has been determined to be essential for cell migration and nervous system development (10, 11). Various functions of CS-2OST have also been identified by several studies. The 2-*O*-sulfation of IdoUA in a highly sulfated chondroitin sulfate B (dermatan sulfate) hexasaccharide sequence has been determined to contribute to heparin cofactor II binding, regulating the blood coagulation cascade (12). In addition, it has been implicated that a polysaccharide structure containing IdoUA(2S)-GalNAc(4S), IdoUA(2S)-GalNAc(6S), or GlcUA(2S)-GalNAc(6S) units exerts potent neurite out-

* This work was supported in part by National Institutes of Health Grants AI50050 and in part by the Intramural Research Program of the NIEHS, National Institutes of Health. The costs of publication of this article were defrayed in part by the payment of page charges. This article must therefore be hereby marked "*advertisement*" in accordance with 18 U.S.C. Section 1734 solely to indicate this fact.

[1] Recipient of a predoctoral fellowship from the American Heart Association MidAtlantic Affiliate.

[2] To whom correspondence should be addressed: Rm. 309, Beard Hall, University of North Carolina, Chapel Hill, NC 27599. Tel.: 919-843-6511; Fax: 919-843-5432; E-mail: jian_liu@unc.edu.

[3] The abbreviations used are: HS, heparan sulfate; CS, chondroitin sulfate; 2-OST, 2-*O*-sulfotransferase; EST, estrogen sulfotransferase; 3-OST-3, 3-*O*-sulfotransferase isoform 3; ST, sulfotransferase; PAPS, 3′-phosphoadenosine 5′-phosphosulfate; PAP, 3′-phosphoadenosine 5′-phosphate; ITC, isothermal titration calorimetry; CDSNS, completely desulfated and *N*-sulfated; dmHS-2OST, *Drosophila* heparan sulfate 2-*O*-sulfotransferase; RPIP-HPLC, reverse-phase ion-pairing HPLC; MBP, maltose-binding protein; h, human; MES, 4-morpholineethanesulfonic acid; PSB, PAPS binding; WT, wild type.

growth-promoting activities. These structural motifs contain 2-*O*-sulfated glucuronic or 2-*O*-sulfated iduronic acid residues, which are biosynthesized by CS-2OST, suggesting an important role of CS-2OST in the development of the mammalian central nervous system (13, 14).

Although HS-2OST and CS-2OST sulfate different polysaccharide substrates, they are strikingly homologous. Human HS-2OST and CS-2OST share 32% identity and 56% similarity in their sulfotransferase (ST) domain. Both enzymes have only one isoform in most of the genome-sequenced organisms (with the exception of fish), in contrast to multiple isoforms for almost all other HS and CS STs. HS-2OST and CS-2OST are also conserved across species. Human HS-2OST shares 75% similarity to insect HS-2OSTs and 67% to *C. elegans* HS-2OST, whereas all vertebrate CS-2OSTs share greater than 85% similarity in the ST domain. HS-2OST transfers the sulfo group from PAPS to the 2-OH position of the hexauronic acid, with a preference for iduronic acid, which is adjacent to an *N*-sulfated glucosamine (GlcNS) residue (15), whereas CS-2OST transfers the sulfo group to the 2-OH position of the hexauronic acid that is adjacent to an *N*-acetylated galactosamine residue (GalNAc) carrying either a 6-*O* or 4-*O* sulfo group (16, 17) (Fig. 1).

In this study, we report a systematic mutagenesis study of HS-2OST and CS-2OST based on their structural homology to other members of the ST superfamily. We have identified six residues in each enzyme that participate in PAPS binding, five residues that potentially mediate substrate binding in HS-2OST, and four residues in CS-2OST. Additionally, we identified two histidine residues that are essential for the catalytic functions of HS-2OST, although one histidine residue was identified in CS-2OST. The unique structural feature in the catalytic sites of HS-2OST and CS-2OST led us identify a homologous protein in *Drosophila*, dmHs2st, as the *Drosophila* HS-2OST. Analysis of the previously suggested HS-2OST from *Drosophila* (18), the gene product of *pipe*, displays neither HS-2OST nor CS-2OST activity.

EXPERIMENTAL PROCEDURES

Preparation of HS-2OST and CS-2OST Bacterial Expression Plasmids (HS-2OST-pET21b and CS-2OST-pET32b)—The catalytic domains of HS-2OST of Chinese hamster (Glu^{28}–Asn^{356}) and human CS-2OST (Asn^{84}–Arg^{406}) were cloned into the pET21b and pET32b vectors (Novagen), respectively, using the EcoRI and HindIII sites to construct a C-terminal His_6-tagged HS-2OST protein and an N-terminal thioredoxin-His_6-tagged CS-2OST fusion protein. The full-length cDNA of hamster HS-2OST and human CS-2OST were gifts from Dr. Rosenberg (Massachusetts Institute of Technology).

Preparation of Drosophila dmHs2st, pip-PA, and pip-PF Bacterial Expression Plasmids—The *Drosophila* cDNA clones encoding dmHs2st (GH20044) and pip-PF (RE07829) were ordered from Open Biosystems (Huntsville, AL), and the cDNA clone encoding for pip-PA (LD12641) was ordered from *Drosophila* Genomics Resource Center (Indiana University). The cDNA fragment encoding for the catalytic domain of dmHs2st (Arg^{39}–Lys^{349}) was amplified and cloned into pET32b vector using EcoRI and SalI sites to generate an N-terminal thioredoxin-His_6-tagged dmHs2st fusion protein. The cDNA fragments encoding for the putative catalytic domain of pip-PA(Met^{106}–Asn^{413}) and pip-PF(Ser^{102}–Phe^{397}) were amplified and cloned into pMAL-c2X vector (New England Biolabs) using the EcoRI and HindIII sites to generate N-terminal maltose-binding protein (MBP)-tagged pipPA as well as pipPF fusion proteins.

Preparation of HS-2OST and CS-2OST Mutants—The mutants of HS-2OST and CS-2OST were prepared using HS-2OST-pET21b and CS-2OST-pET32b as the templates, respectively, and a method modified from Stratagene Quickchange mutagenesis kit has been described elsewhere (19). The primers for preparing mutants were synthesized by Invitrogen. The resultant constructs were sequenced to confirm the anticipated mutation (University of North Carolina Genomic Analysis Facility).

Expression and Purification of HS-2OST and CS-2OST Proteins—The expression plasmids for various mutants or wild type were carried out in Origami-B cells (Novagen) carrying pGro7 (Takara, Japan) plasmid expressing chaperonin proteins GroEL and GroES of *Escherichia coli*. Transformed cells were typically grown in 100 ml of LB medium supplemented with 12.5 μg/ml tetracycline, 15 μg/ml kanamycin, 35 μg/ml chloramphenicol, and 50 μg/ml carbenicillin at 37 °C. When the A_{600} reached 0.4–0.7, isopropyl β-thiogalactopyranoside (at the final concentration of 0.15 mM) and L-arabinose (at the final concentration of 1 mg/ml) were added to induce the expression of HS-2OST (or CS 2-OST) and chaperonin proteins, respectively. Then the cells were allowed to shake overnight at 22 °C. Cells were pelleted and resuspended in 8 ml of a buffer containing 25 mM Tris, pH 7.5, 500 mM NaCl, and 30 mM imidazole. Cells were disrupted by sonication then spun down as described (20), and the supernatant was applied to a 1-ml Ni-Sepharose 6 fast flow (Amersham Biosciences) column at a flow rate of 1 ml/min. The purified proteins were eluted from the column with a linear gradient of imidazole from 30 to 300 mM in 15 ml. The purity of the resultant proteins was typically greater than 80% for HS-2OST and between 50 and 90% pure for CS-2OST as determined by 10% SDS-PAGE (Bio-Rad). About 0.5–2-liter cultures were used to obtain sufficient amount of proteins for the analysis by isothermal titration calorimetry (ITC) or 3′,5′-ADP (PAP)-agarose chromatography (Sigma).

Expression and Purification of dmHs2st, pip-PA, and pip-PF—The expression vectors of dmHs2st, pip-PA, and pip-PF were prepared as described above. The purification method of dmHs2st is identical to that of HS-2OST, whereas MBP-pip-PA and MBP-pip-PF were purified using a method described previously (21).

Determination of the Sulfotransferase Activity—Sulfotransferase activity was determined by incubating 200 ng of purified mutant or wild type HS-2OST proteins with 10 μg of completely desulfated *N*-sulfated (CDSNS) heparin (gift from Dr. Linhardt, RPI) and $2–5 \times 10^5$ cpm of [^{35}S]PAPS (10 μM) in 50 μl of buffer containing 50 mM MES, pH 7.0, 10 mM $MnCl_2$, 5 mM $MgCl_2$, and 1% Triton X-100. The reaction was incubated at 37 °C for 30 min and quenched by the addition of 6 M urea and 100 mM EDTA. The sample was then subjected to a 200-μl DEAE-Sepharose chromatograph to purify the [^{35}S]HS. The quantity of [^{35}S]HS was then determined by liquid scintillation

counting. The procedures determining the activity of CS-2OST were essentially identical to those of HS-2OST, except the substrate used in the assay is dermatan sulfate (porcine skin; Sigma). For substrate specificity measurement of HS-2OST and CS-2OST, the CDSNS heparin and the *N*-sulfoheparosan were pretreated with chondroitinase ABC, whereas the chondroitin sulfate A and C (Sigma) and dermatan sulfate were pretreated with heparin lyases in order to eliminate potential cross-contamination between heparin and chondroitin sulfates.

Determination of the Binding Constant (K_D) of HS-2OST to PAP by ITC—ITC was performed on a MicroCal VP-ITC. Solutions were cooled to 20 °C and degassed under vacuum before use. Experiments were conducted using 20–30 μM protein in 100 mM phosphate buffer, pH 7.0, 300 mM NaCl, 100 mM arginine, and 100 mM glutamate at 20 °C. Titrations were performed by injecting 5 μl of 0.7 mM PAP (Sigma) in the same buffer. Data analysis was completed using Origin software.

Determination of PAP Binding Affinity Using PAP Chromatography—PAP-agarose affinity chromatography was used to determine the binding affinity of the wild type and mutant proteins of CS-2OST to PAP using an AKTA-FPLC system (Amersham Biosciences). Approximately 300 μg of proteins in 5 ml of a buffer containing 20 mM Tris, pH 8.2, and 100 mM NaCl (buffer A) was loaded onto a PAP-agarose column (7 × 52 mm) pre-equilibrated with buffer A at a flow rate of 0.5 ml/min. Unbound material was removed by washing with 8 ml of buffer A. Bound proteins were eluted with a linear gradient of NaCl from 0.1 to 1.5 M in 15 ml, and the eluent was monitored by $A_{280\ nm}$. The NaCl concentration at the central position of the eluted CS-2OST peak was recorded as the elution concentration.

Disaccharide Analysis of 2-O-[^{35}S]HS—The 2-*O*-[^{35}S]HS prepared from HS-2OST- and dmHs2st-modified HS was degraded with nitrous acid at pH 1.5 followed by reduction with sodium borohydride (22). The disaccharides were resolved by a C18-reversed phase column (0.46 × 25 cm) (Vydac) under the reverse-phase ion-pairing HPLC (RPIP-HPLC) condition (23). The identities of the disaccharides were determined by coeluting with appropriate ^{3}H-labeled IdoUA2S-AnMan (23), where AnMan represents 2,5-anhydromannitol.

RESULTS

Substrate Specificities of HS-2OST and CS-2OST

The catalytic domains of HS-2OST and CS-2OST were expressed in *E. coli*. The substrate specificities of HS-2OST and CS-2OST were determined using five different polysaccharide substrates. As shown in Table 1, HS-2OST exhibited excellent activity toward CDSNS heparin (94.7 pmol/μg of substrate) and moderate activity toward *N*-sulfoheparosan (9.3 pmol/μg), although it showed no activity toward chondroitin sulfate A and C, and only trace amounts of activity toward chondroitin sulfate B (0.4 pmol/μg). CS-2OST showed the best activity toward chondroitin sulfate A (61.2 pmol/μg) and chondroitin sulfate B (31.1 pmol/μg) and moderate activity toward chondroitin sulfate C (16.9 pmol/μg), and it displayed only trace amounts of activity toward CDSNS heparin and *N*-sulfoheparosan. The structures of the disaccharide repeating unit of the polysaccharide substrates are shown in Fig. 1*B*. It is important to note that the observed CS-2OST substrate profile is largely consistent with the one described in a recent report where CS-2OST was expressed in COS-7 cells, observing that the chondroitin sulfate A is the best substrate among tested chondroitin/dermatan sulfates (17). However, our results showed that chondroitin sulfate B (dermatan sulfate) can also serve as a substrate for CS-2OST, which is consistent with another report on the substrate specificity of CS 2-OST expressed in insect cells (16). Taken together, our results suggest that bacterially expressed recombinant proteins specifically transfer the sulfo group to the hexauronic acid that is linked to GlcNS residue (for HS-2OST) and GalNAc residue (for CS-2OST), respectively, as illustrated in Fig. 1*A*.

TABLE 1
Substrate specificities analysis of HS-2OST and CS-2OST

Substrates[a]	Sulfate transferred by HS-2OST	Sulfate transferred by CS-2OST
	pmol/μg	*pmol/μg*
CDSNS heparin	94.7	1.4
N-Sulfoheparosan	9.3	0.7
Chondroitin sulfate A	<0.1	61.2
Chondroitin sulfate B	0.4	31.1
Chondroitin sulfate C	<0.1	16.9

[a] The structures of the disaccharide repeating unit of the polysaccharide substrates are shown in Fig. 1*B*.

The PAPS-binding Sites of HS-2OST and CS-2OST

The PAP-binding Site of HS-2OST—Based on the structures of estrogen sulfotransferase (EST) and HS 3-OSTs, we built a homology model of HS-2OST (Fig. 2*A*). A set of amino acid residues in HS-2OST was identified to be involved in the hydrogen bonding with PAPS. The residues predicted to contribute to the binding to the 5′-phosphosulfate group of PAPS include the following: Lys^{83}, Thr^{84}, Ser^{86}, and Thr^{87} (Fig. 2*B*). Each of these residues was then mutated to alanine to test how the mutations affected the enzymatic activity (Table 2). The mutants exhibited impaired activities but to different extents. The K83A and S86A mutations abolished the activity, whereas T87A and T84A show less potent but noticeable impairment to the activity. As expected, the mutant proteins do not bind to PAP as determined by ITC (Table 2), suggesting that the loss or significant impairment of the sulfotransferase activity is because of the decrease in the binding affinity to PAPS.

Residues involved in binding to the 3′-phosphate group of PAPS were identified to be Arg^{164} and Ser^{172} (Fig. 2*B*). The alanine mutants of these two residues showed significantly decreased enzymatic activity, and the binding affinity to PAP is abolished as determined by ITC. These results suggest that both Arg^{164} and Ser^{172} are involved in binding to PAPS.

PAP is the product of sulfotransferase-catalyzed reactions. Because of the chemical instability of PAPS, we only measured binding affinity of the mutated HS-2OST to PAP, provided that this approach was used for characterizing 3-OST-1 (20). Furthermore, the K_m value of wild type HS-2OST toward PAPS was determined to be 18.5 μM, which is very close to the binding affinity to PAP (K_D = 17.3 μM), suggesting that this approach is applicable to HS-2OST.

PAPS-binding Site of CS-2OST—Because CS-2OST and HS-2OST have very homologous amino acid sequences, the

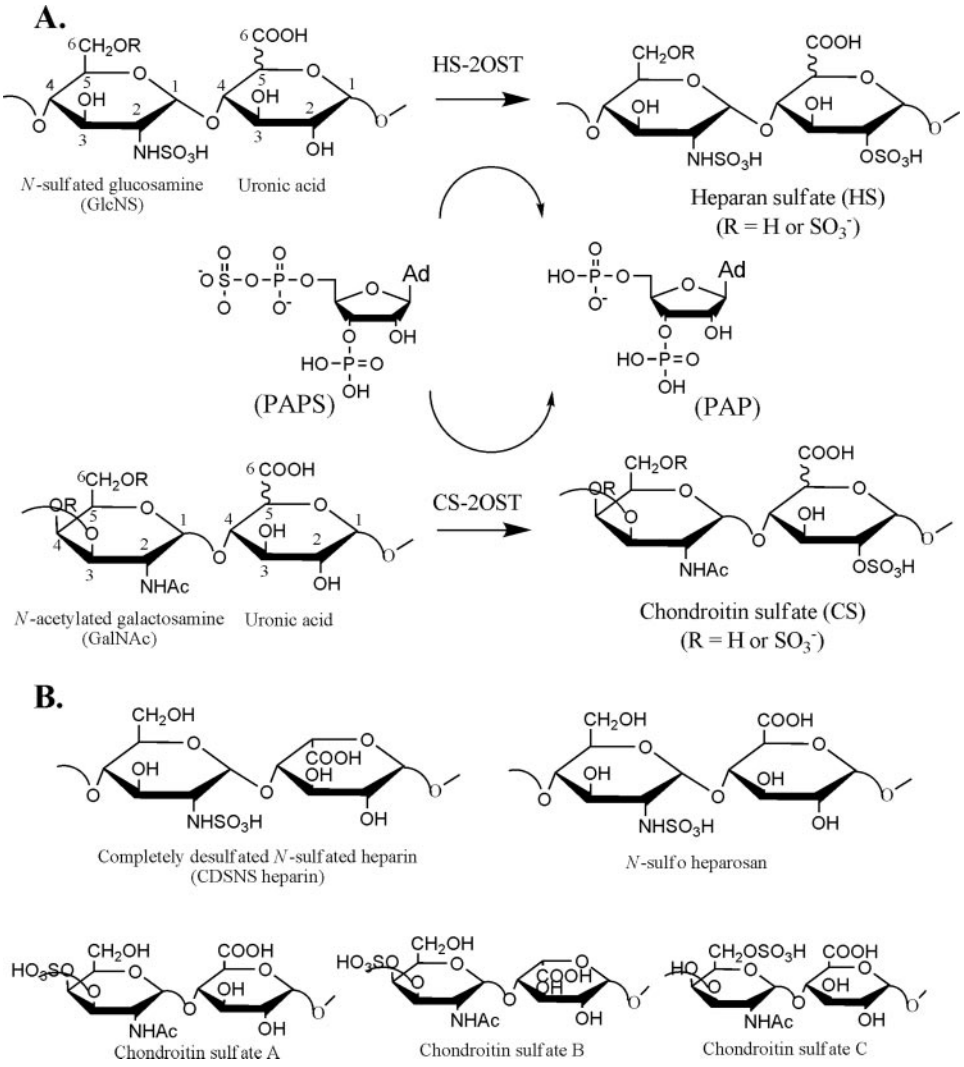

FIGURE 1. **Reactions catalyzed by HS-2OST and CS-2OST and the structures of the disaccharide repeating units of polysaccharide substrates.** *A* shows the reactions catalyzed by HS-2OST as well as catalyzed by CS-2OST. *B* shows the structures of the disaccharide repeating units of the polysaccharide substrates used in this study.

residues involved in binding to the 5′-phosphosulfate in CS-2OST are believed to be those corresponding residues in HS-2OST as described above. The residues in CS-2OST include Lys[112], Cys[113], Ser[115], and Arg[116] (see Fig. 2*B* for the amino acid sequence alignment). The residues were mutated to alanine, and the mutants showed diminished sulfotransferase activity in a very similar pattern to that observed for the HS-2OST mutants (Table 2). Because the solubility of CS-2OST is low, we could not determine the binding affinity (K_D) to PAP using ITC. Instead, we decided to estimate the binding affinity of the mutant to PAP using PAP-agarose affinity chromatography eluted with a concentration gradient of NaCl (20). All tested mutants were eluted from the PAP column at a lower concentration compared with the wild type protein (Table 2), suggesting that mutation at these residues decreased binding affinity to PAP.

Both Arg[189] and Ser[197] are predicted to bind to the 3′-phosphate of PAPS based on the homology alignment (Fig. 2*B*). Indeed, mutants R189A and S197A displayed diminished enzymatic activity and reduced binding affinity to PAP (Table 2).

Catalytic Residues of HS-2OST and CS-2OST

It has been suggested that a catalytic base is beneficial for facilitating the deprotonation of the acceptor substrate to allow the sulfotransfer reaction to occur (24). A structural neighbor search of HS-2OST and CS-2OST through GenTHREADER (25) reveals that the enzymes are structurally more similar to human EST than to HS 3-OSTs, especially in the β7 region of EST (Fig. 2*B*). Within this region, the catalytic base of EST, His[107], aligns with His[142] of HS-2OST and His[168] of CS-2OST, suggesting that His[142] and His[168] may serve as a catalytic base for HS-2OST and CS-2OST, respectively. Indeed, His[142] is conserved among all HS-2OST from different species and so is His[168] in CS-2OST, suggesting that they are essential for enzymatic activities.

His[142] and His[140] in HS-2OST—To address the role of His[142] in HS-2OST, a H142A mutant was prepared. This mutant retained around 5% of the wild type HS-2OST activity rather than completely abolishing the activity (Table 3), suggesting other residues may be involved in the deprotonation step. Based on the homology model, His[140] may also be located near the catalytic site and have a similar distance between the sulfo group of PAPS and the acceptor site His[142] (as illustrated in Fig. 3). Further investigation found that the corresponding residue of EST, Lys[105], has been suggested to play a role in the catalysis of EST (26). Like His[142], His[140] in HS-2OST is also conserved across species, suggesting that this residue is critical for the sulfotransferase activity. An H140A mutant was prepared and exhibited about 4% of the WT HS-2OST activity (Table 3). To this end, a H140A/H142A double mutant was prepared, and indeed, this mutant resulted in a complete loss of HS-2OST activity (<1%) (Table 3). To rule out the possibility that His[140] and His[142] bind to PAPS, the mutants H140A, H142A, and H140A/H142A were subjected to ITC analysis. The result indicated that all of the mutants retained similar PAP binding affinity to that of WT HS-2OST protein (Table 3). Taken together, the results suggest that both histidines are important for the activity of HS-2OST.

Role of His[168] in CS-2OST—The mutation at His[168] in CS-2OST that corresponds to His[107] in hEST resulted in a complete loss of sulfotransferase activity (Table 3). The binding affinity of H168A mutant to PAP was also estimated by subject-

ing to a PAP-affinity column. The mutant H168A and wild type CS-2OST eluted at similar salt concentrations suggesting they have very similar binding affinity for PAP. These results support the hypothesis that His^{168} is a potential catalytic base for the CS-2OST. Residues Thr^{166} and Arg^{167} that are proximate to His^{168} were also tested for contributions to catalysis because they align close to His^{140} in the sequence of HS-2OST. T166A and R167A displayed similar or moderately decreased sulfotransferase activity compared with wild type (Table 3), suggesting both residues are nonessential for catalysis.

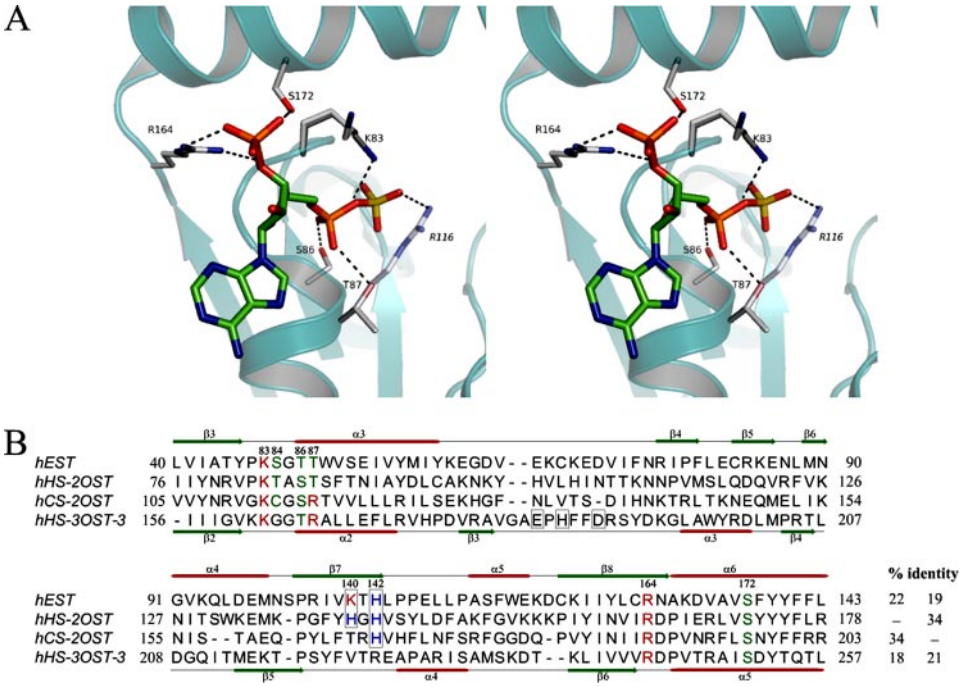

FIGURE 2. **PAPS-binding sites of HS-2OST and CS-2OST.** *A,* stereo diagram of the PAPS-binding sites of HS-2OST and CS-2OST. Model of the PAPS-binding site is generated by using the hEST-PAPS Protein Data Bank coordinates from 1HY3. Ser^{86} of HS-2OST and Arg^{116} (shown as *transparent stick*) of CS-2OST are modeled in by replacing the Thr^{50} and Thr^{51} of hEST, respectively. Possible hydrogen bonds between the side chains and PAPS are shown as *black dots*. The sulfur atom is shown in *yellow* and the phosphor atom is shown in *orange*. Two conformation states of Lys^{83} (Lys^{47} in hEST) were shown as in hEST-PAPS structure (*white stick*, pointing away from PAPS), and in hEST-PAP structure (*gray stick*, pointing toward PAP). *B,* partial sequence alignment of hEST, hHS-2OST, hCS-2OST, and hHS-3OST-3 showing sequences roughly from the 3′-phosphate PAP-binding site to the 5′-phosphate PAP-binding site. The secondary structures of hEST (*top*) and hHS-3OST-3 (*bottom*) are shown in the following: α-helix in *red tube*, β-strand in *green arrow*, and coil in *gray line*. The residues that involve in PAP binding are colored, and the catalytic residues of each enzyme are *boxed*. The PAP-binding residues and catalytic residues are numbered as in hHS-2OST. The percentage of amino acid identity with hHS-2OST and hCS-2OST within the region shown is displayed in the *bottom right corner* of this figure.

Substrate-binding Residues of HS-2OST and CS-2OST

Our efforts for identifying potential substrate-binding residues of HS-2OST and CS-2OST are largely based on their structural homology to the structure of the ternary complex of HS 3-OST-3 with PAP and bound tetrasaccharide (27). HS 3-OST-3 interacts with the substrate mainly through the following three regions: around the loop that binds to the 5′-phosphate group of PAPS between β2 and α2 (Fig. 4, *magenta*); at and after α-helix 5 (*yellow*); and the long coil before α-helix 11 (*blue*). Mutagenesis was conducted to examine possible roles for these residues in substrate binding by HS-2OST and CS-2OST.

Roles of Arg^{80} in HS-2OST and Arg^{109} in CS-2OST—In the PSB loop region of HS 3-OST-3 (between β2 and α2), a lysine residue (Lys^{161}) is involved in binding the carboxyl group of the iduronic acid of the tetrasaccharide substrate (Fig. 4, *magenta*) (27). The corresponding residue in HS-2OST is Arg^{80}. Mutation at Arg^{80} (R80A) of HS-2OST indeed reduced the sulfo-

TABLE 2
Analysis of HS-2OST and CS-2OST mutants defective in PAPS binding

HS-2OST mutants	Activity level	Expression level	PAP K_D	CS-2OST mutants	Activity level	Expression level	PAP column elution salt concentration
	%	%	μM		%	%	mM
WT	100	100	17.3 ± 1.9	WT	100	100	1100
K83A	<1	50	ND[a]	K112A	<1	30	780
T84A	12 ± 2	50	ND	C113A	15 ± 5	70	690
S86A	<1	100	ND	S115A	<1	85	820
T87A	6 ± 3	75	ND	R116A	2 ± 1	85	730
R164A	3 ± 2	100	ND	R189A	<1	100	630
S172A	7 ± 1	100	ND	S197A	7 ± 2	110	730

[a] ND indicates not detectable under the conditions used, usually has a K_D value greater than 200 μM.

TABLE 3
Analysis of HS-2OST and CS-2OST mutants defective in the catalytic function

HS-2OST Mutants	Activity level	Expression level	PAP K_D	CS-2OST mutants	Activity level	Expression level	PAP column elution salt concentration
	%	%	μM		%	%	mM
WT	100	100	17.3 ± 1.9	WT	100	100	1100
H140A	4 ± 1	120	22.8 ± 1.5	*T166A*	100	70	NA[a]
H142A	5 ± 2	150	13.8 ± 0.8	*R167A*	22 ± 2	70	NA
H140A/H142A	<1	100	24.6 ± 2.3	H168A	<1	130	1180

[a] NA indicates not applicable.

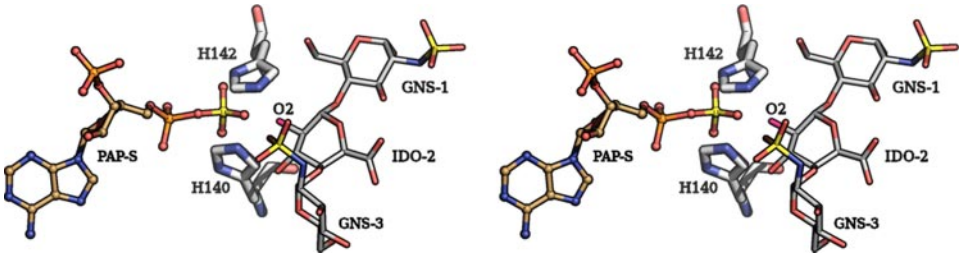

FIGURE 3. **Stereo diagram of the catalytic site of HS-2OST.** The catalytic site of HS-2OST was created by taking the hEST-PAPS coordinates (Protein Data Bank code 1HY3) and the HS sugars 1–3 from the HS 3-OST-3 coordinates (Protein Data Bank code 1T8U). The trisaccharide was then moved around until the 2-OH of the iduronic acid was sitting at the original position of the 3-OH of the glucosamine in the HS 3-OST-3. The 6-*O*-sulfate groups was removed from the GNS-1 (*N*-sulfoglucosamine 1) and GNS-3 (*N*-sulfoglucosamine 3) for easy viewing. The His^{140} of HS-2OST was modeled by replacing the Lys^{105} of hEST with a common rotomer of the histidine side chain. The sulfate acceptor 2-OH group of IDO-2 (iduronic acid) is labeled and shown in *magenta*. Sulfur is shown in *yellow*. The structure diagram is generated by PyMOL.

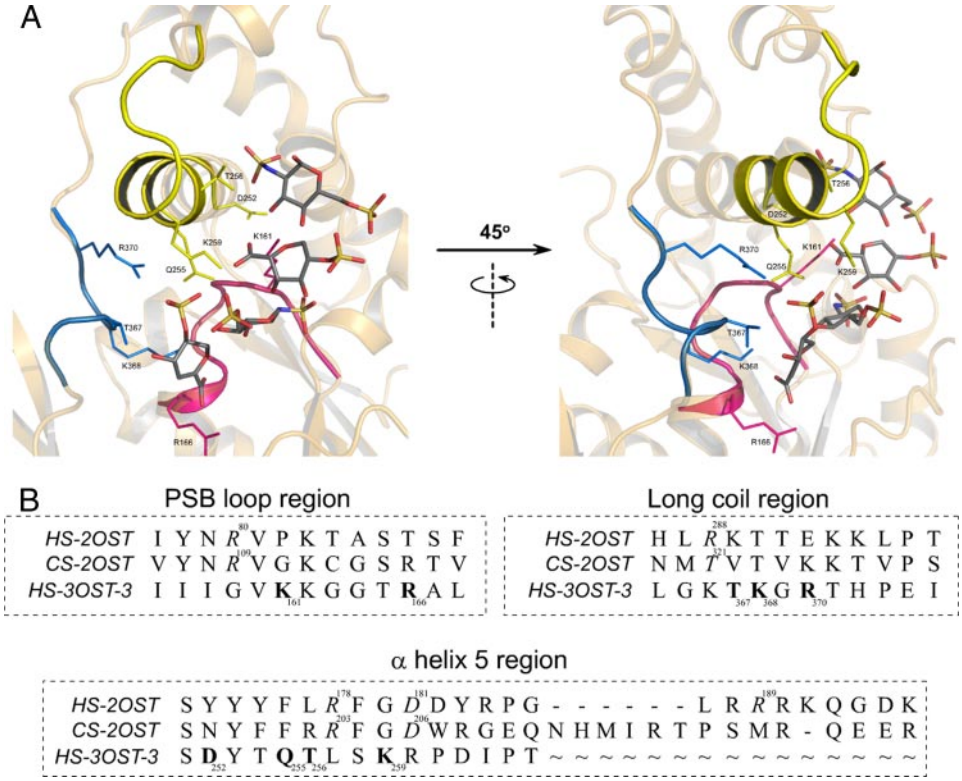

FIGURE 4. **The substrate-binding regions of HS 3-OST-3, whose homologous regions were studied in HS-2OST and CS-2OST.** *A,* three main substrate-binding regions of HS 3-OST-3 are shown in the schematic diagram using the coordinates from the HS 3-OST-3-PAP-tetrasacchride complex (Protein Data Bank code 1T8U). The PAPS-binding (PSB) loop is shown in *magenta* (where Arg^{80} of HS-2OST resides); the region after α-helix 5 is shown in *yellow* (where Arg^{178}, Asp^{181}, and Arg^{189} of HS-2OST reside), and the long coil region before α-helix 11 is shown in *blue* (where Arg^{288} of HS-2OST resides). The side chains of the residues in HS 3-OST-3 that make direct contact with the tetrasaccharide substrate are shown as a *thin line* and labeled. Tetrasaccharide is shown as a *gray stick*. The structure diagram is generated by PyMOL. *B,* sequence alignments of the HS-2OST, CS-2OST, and HS 3-OST-3 in the above mentioned regions are shown separately in the *dashed boxes*. The studied residues in HS-2OST and CS-2OST are shown in *italics*, and the residue numbers are labeled as *superscripts*. The residues in HS 3-OST-3 that make direct contact with the substrate are shown in *boldface type*, and the residue numbers are labeled as *subscripts*. The introduced gaps are shown as *dashes*. Part of the sequence of HS 3-OST-3 in α-helix 5 region is replaced by ~ because it has no homology to HS-2OST and CS-2OST.

transferase activity to about 2.5% of the wild type level (Table 4). In addition, the results from ITC analysis demonstrated that R80A binds to PAP with a K_D of 19.7 μM, very close to the K_D of WT HS-2OST at 17.3 μM (Table 4), suggesting that the decrease of the sulfotransferase activity in the R80A mutant is not because of the decreased affinity for PAP.

In a similar experiment, the R109A mutant of CS-2OST (the corresponding residue for Arg^{80} in HS-2OST) displayed about 4% of the sulfotransferase activity. Again, this loss in activity is unlikely because of the reduced PAPS binding as both R109A mutant and wild type proteins have similar affinity to PAP as determined by the PAP-affinity column (Table 4).

Roles of Arg^{178} and Asp^{181} in HS-2OST—In HS-2OST, Arg^{178}and Asp^{181} are located right after the 3′-phosphate PAPS-binding region (Fig. 4, *yellow*), where several contacts with the tetrasaccharide substrate have been identified in HS 3-OST-3 (α-helix 5) (27). We hypothesize that both Arg^{178} and Asp^{181} may interact with the substrate of HS-2OST. In addition, Arg^{178} and Asp^{181} are conserved in all vertebrate and invertebrate HS-2OST. The mutants R178A and D181A show significant decrease in the sulfotransferase activity, although the extent of the effect by mutation at Arg^{178} appears to be greater (Table 4).

The binding affinities to PAP of these mutants were determined by ITC. The ITC analysis showed that D181A binds to PAP with a K_D of 14.4 μM, which is very similar to wild type protein, whereas R178A binds to PAP noticeably weaker with a K_D at 101.5 μM. The role of Asp^{181} could form the hydrogen bond with the OH of the substrate as demonstrated for Asp^{252} of HS 3-OST-3 (27). The role of Arg^{178} could be involved in interacting with the substrate as well as stabilizing the structure that binds to PAPS. Indeed, the weaker binding affinity of R178A to PAP could be explained by destabilization of helix 5 consequently affecting the orientation of Ser^{172} that binds to the 3′-phosphate of PAPS.

The Roles of Arg^{203} and Asp^{206} in CS-2OST—Arg^{203} and Asp^{206} in CS-2OST align with Arg^{178} and Asp^{181} in HS-2-OST (Fig. 4*B*). Residues Arg^{203} and Asp^{206} are conserved in CS-2OST from different species. Mutants R203A and D206A of CS-2OST displayed severe defects in sulfotransferase activity (Table 4). Both R203A and D206A mutants were eluted at 900 and 940 mM NaCl from the PAP-

TABLE 4
Analysis of HS-2OST and CS-2OST mutants potentially defective in substrate binding

HS-2OST Mutants	Activity level	Expression level	PAP K_D	CS-2OST mutants	Activity level	Expression level	PAP column elution salt concentration
	%	%	μM		%	%	mM
WT	100	100	17.3 ± 1.9	WT	100	100	1100
R80A	2.5 ± 0.5	80	19.7 ± 1.9	R109A	4 ± 1	170	1170
R178A	2 ± 1	80	101.5 ± 12	R203A	<1	20	900
D181A	9 ± 2	60	14.4 ± 0.2	D206A	<1	130	940
R189A	4 ± 0.5	100	13.4 ± 0.5	*R221A*	100	100	NA[a]
R288A	7 ± 2	100	7.8 ± 0.7	T321A	9 ± 2	90	970
R288T	1.5 ± 0.5	100	ND[b]	T321R	3 ± 1	80	950

[a] NA indicates not applicable.
[b] ND indicates not detectable under the condition used, usually has a K_D value greater than 200 μM.

affinity column, showing that both mutants have somewhat decreased binding affinity for PAP compared with the wild type protein (Table 4). However, the mutants that are defective in PAPS binding were typically eluted on average at 730 mM NaCl from the column, suggesting that the complete loss of sulfotransferase activity of R203A and D206A is not solely because of the decreased binding affinity to PAPS.

Role of Arg^{189} in HS-2OST—Arg^{189} is located in a region following helix 5 of HS 3-OST-3 (Fig. 4, *yellow*), which is dissimilar between HS-2OST and CS-2OST. We speculate that this region may play a role in contributing to the substrate specificity between the two enzymes. In this region, HS-2OST is shorter and contains a stretch of four basic residues, Arg-Arg^{189}-Arg-Lys, whereas CS-2OST is longer and does not contain consecutive basic residues (Fig. 4*B*). By mutating each of these four basic residues in HS-2OST to alanine, we found only the mutant R189A significantly reduced the HS-2OST activity (Table 4). All other mutations retained higher than 50% of the activity of wild type protein (data not shown). In addition, R189A has binding affinity (13.4 μM) toward PAP comparable with that of wild type protein (17.3 μM), suggesting that the loss of activity of R189A is not because of impaired PAP binding to the enzyme. Furthermore, we also found that Arg^{189} is completely conserved ranging from *C. elegans* to human, implicating the indispensable function of this residue for the enzymatic activity of HS-2OST. Arg^{221} in CS-2OST is a basic residue in this region. However, the R221A mutant displayed the same activity as the wild type CS-2OST, suggesting that this residue is nonessential for the activity of CS-2OST. Together, our data suggest that Arg^{189} interacts with the substrate of HS-2OST.

Specific Roles of Arg^{288} of HS-2OST and Thr^{321} of CS-2OST—Like HS 3-OST-3, HS-2OST and CS-2OST have a long coil region that is immediately ahead of the last extended helix based on structure prediction (Fig. 4, *blue*). In HS 3-OST-3, this region contains several residues, including Thr^{367}, Lys^{368}, and Arg^{370}, which interact with the nonreducing end saccharide unit of the acceptor. HS-2OST contains a basic Arg^{288} that may interact with the HS substrate. The R288A mutant had significantly impaired enzymatic activity of HS-2OST but maintained a similar binding affinity to PAP as that for wild type protein (Table 4). The corresponding mutation in CS-2OST, T321A, had a similar effect on CS-2OST activity even though it showed a moderate decrease in PAP binding (Table 4), presumably resulting from an indirect influence on PAPS binding.

Further mutational analysis at Arg^{288} in HS-2OST and Thr^{321} in CS-2OST revealed the specific needs of the residues for the respective sulfotransferase activities. To test whether Arg and Thr are interchangeable for HS-2OST and CS-2OST at this position, we prepared an R288T mutation in HS-2OST and a T321R mutation in CS-2OST, and we found that both R288T and T321R lost the activity of their respective enzymes (Table 4). These observations suggest that Arg^{288} is specifically needed for HS-2OST to interact with the HS polysaccharide substrate, whereas Thr^{321} is specifically needed for CS-2OST to interact with the CS polysaccharide substrate. We observed differential effects of R288T and T321R mutants on PAP binding. Mutant R288T resulted in undetectable binding to PAP, whereas T321R has moderate effect on the binding to PAP (Table 4). We noted that this area interacts with both PAPS and substrate in HS 3-OST-3. Thus, disruption of the coil could affect PAPS binding affinity. A similar effect has been observed for Arg^{370} of HS 3-OST-3 as the nitrogen of the backbone of this residue interacts with the phosphate of PAPS (27).

The representative data from the analysis of the binding of PAP and HS-2OST and mutants are shown in Fig. 5. The summary of the thermodynamic parameters of wild type and mutants of HS-2OST are presented in Table 5.

Characterization of Drosophila Heparan Sulfate 2-O-Sulfotransferase (dmHS-2OST)

Drosophila pipe gene expression in the follicle cells has been demonstrated to be essential for the establishment of the dorsal-ventral polarity of the future embryo (18, 28, 29). Because *pipe* encodes a family that bears around 20–25% identity to the ST domain of human HS-2OST, it has been widely speculated that *pipe* encodes for an enzyme that has HS-2OST activity. However, there is no direct evidence suggesting that the gene product of *pipe* has HS-2OST activity. Interestingly, another *Drosophila* gene *Hs2st* has also been suggested to encode for the *Drosophila* HS-2OST (dmHS-2OST), sharing 59% identity to the ST domain of human HS-2OST (16). We decided to determine whether the *pipe* or *Hs2st* gene products have the activities of HS-2OST and CS-2OST.

Comparing the distribution of the key amino acid residues for HS-2OST with *Drosophila* proteins suggests that dmHs2st is equivalent to HS-2OST. From the alignment of the three sequences, we noticed that pip-PA, pip-PF (two gene products of *pipe* with 60% homology), and dmHs2st (gene product of *Hs2st*) contains the well conserved PAPS-binding region and also the four invariable cystines in the flexible region (Fig. 6). However, two major differences suggest dmHs2st is the best candidate for *Drosophila* HS-2OST. First, at the catalytic site,

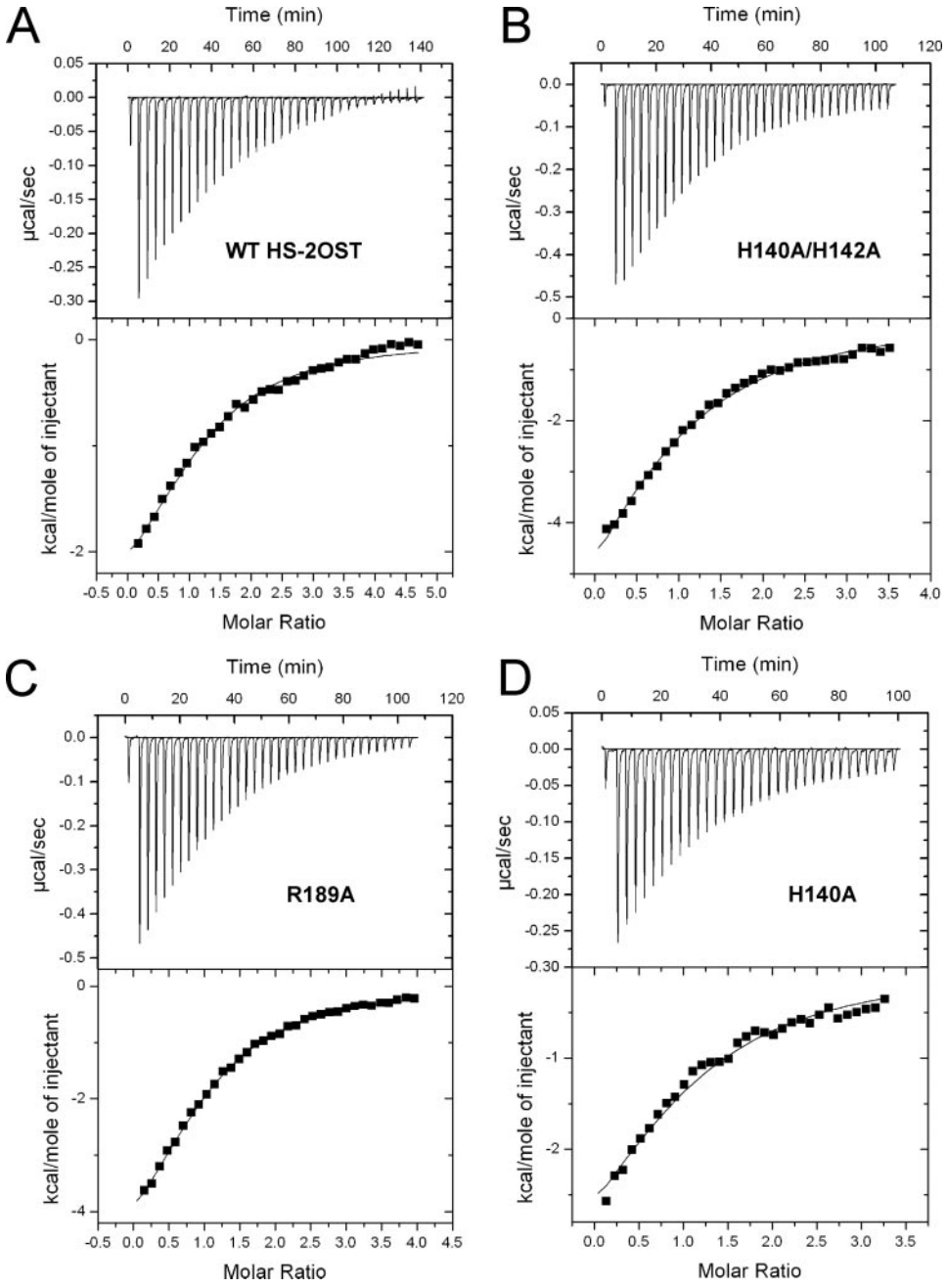

FIGURE 5. **Representative ITC data for the interaction of PAP and WT HS-2OST or HS-2OST mutants.** ITC data for WT HS-2OST (*A*), mutant H140A/H142A (*B*), R189A (*C*), and H140A (*D*) are shown. In each figure, the heat changes associated with titration of PAP into the enzyme are shown in the *upper panel*, and the integrated binding isothermal curve is shown in the *bottom panel*. The isothermal curve was fitted to a one-site model. The derived thermodynamic parameters are presented in Table 5.

dmHs2st contains two histidines that align with His^{140} and His^{142} of HS-2OST, whereas pip-PA/PF only has one histidine around this position. Second, we found dmHs2st contains an aspartic acid at the position of Asp^{181} in HS-2OST, whereas pip-PA/PF has a tryptophan/leucine at the same positions (Fig. 6). As described above, His^{140}, His^{142}, and Asp^{181} are critical for the activity of HS-2OST.

To test this experimentally, we successfully expressed an N-terminal thioredoxin-His_6-tagged fusion protein of dmHs2st (renamed as dmHS-2OST) in *E. coli*. The sulfotransferase activity and substrate specificity were determined. By comparing the susceptibility of dmHS-2OST to various polysaccharide substrates, including CDSNS heparin, chondroitin, and chondroitin sulfate A, B, and C, we found that dmHS-2OST displayed essentially the same substrate specificity as hamster HS-2OST, with an enzymatic activity exclusively for CDSNS heparin (60 pmol/μg). Furthermore, disaccharide analysis of dmHS-2OST-modified CDSNS heparin demonstrated that it contained the ^{35}S-labeled disaccharide with a structure of [2-*O*-^{35}S] IdoUA2S-AnMan, a characteristic disaccharide product resulting from 2-OST-modified CDSNS heparin (Fig. 7). Thus, dmHS-2-OST specifically transfers a sulfo group to the 2-OH position of IdoUA residue (Fig. 7). To this end, our results suggest that the gene product of *hs2st*, dmHs2st, is the *Drosophila* HS-2OST.

Meanwhile, we also successfully expressed two gene products of *pipe*, pip-PA and pip-PF, in the form of N-terminally tagged MBP. The resulting MBP-pipPA and MBP-pipPF, even though expressed in large quantity and appearing to be very soluble, failed to show any HS- or CS-sulfotransferase activities toward the substrates tested, including CDSNS heparin, chondroitin, and chondroitin sulfate A, B, and C.

DISCUSSION

Since the molecular cloning of HS-2OST and CS-2OST in the late 1990s, there have been numerous studies addressing their substrate specificities, physiological functions, and even their interaction with other proteins (10, 11, 15–17, 30, 31). Unfortunately, there have been no studies addressing structural features and mechanism of action, which greatly impeded our further understanding of the detailed biochemistry of these two important enzymes. Here we report the mutational study of HS-2OST and CS-2OST to reveal the PAPS-binding residues, the potential catalytic residues, and substrate-binding residues. The predicted secondary structures and residues with identified functions for HS-2OST and CS-2OST are summarized in Fig. 8.

The PAPS-binding sites of HS-2OST and CS-2OST are similar to those of the previously characterized sulfotransferases;

TABLE 5

Summary of the thermodynamic parameters of the binding of PAP to wild type and mutated HS-2OST as determined by ITC

Protein	K_D	No. of binding sites (n)	ΔH	ΔS
	μM		*cal/mol*	*cal/mol*
WT HS-2OST	17.3 ± 1.9	1.13 ± 0.07	−3203 ± 246.4	10.9
H140A	22.8 ± 1.5	1[a]	−4898 ± 125.5	4.54
H142A	13.8 ± 0.8	0.89 ± 0.03	−5830 ± 239.1	2.35
H140A/H142A	24.6 ± 2.3	0.81 ± 0.08	−10520 ± 1196	−14.8
R80A	19.7 ± 1.9	0.95 ± 0.06	−2757 ± 229.3	12.2
R178A	101.5 ± 12	1[a]	−3754 ± 268.4	5.5
D181A	14.4 ± 0.2	1[a]	−1773 ± 103.0	16.1
R189A	13.4 ± 0.5	0.98 ± 0.02	−6142 ± 164.5	1.35
R288A	7.8 ± 0.7	0.87 ± 0.03	−4347 ± 208.0	8.58

[a] During the curve fitting of these mutants, the value of n is fixed to 1 to give more accurate estimation of K_D.

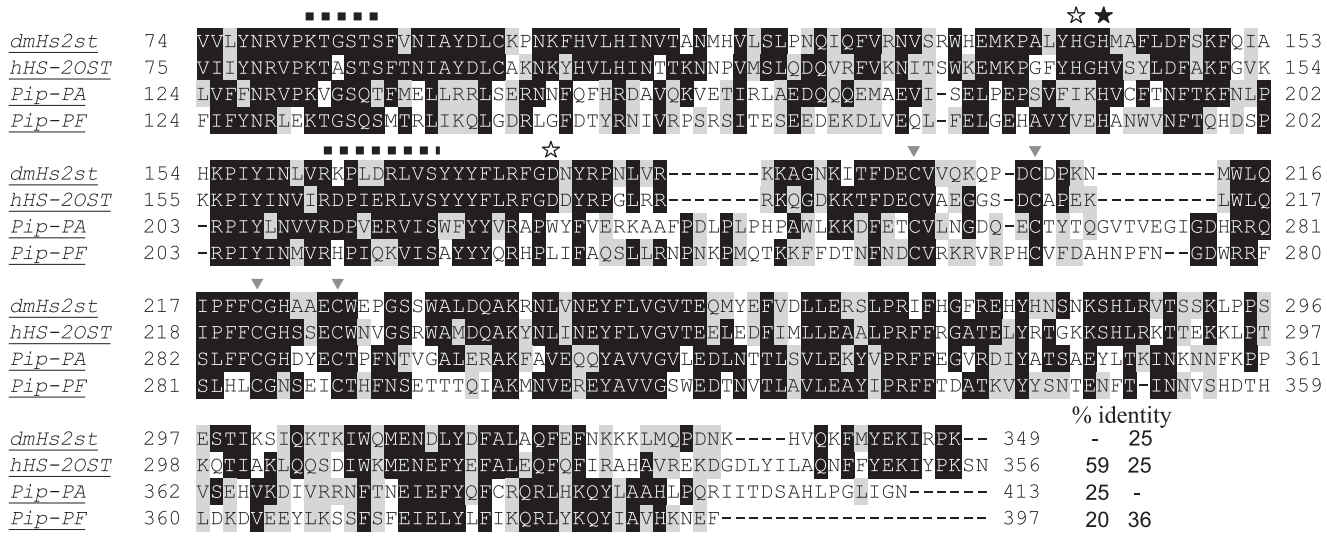

FIGURE 6. **Multiple amino acid sequence alignment of the human HS-2OST and the *Drosophila* Hs2st, Pip-PA, and Pip-PF.** The aligned amino acids are *boxed* and *shaded black* for identical residues and *gray* for similar residues, and the introduced gaps are shown as *dashes*. The His[142] of hHS-2OST is marked by ★, and the His[140] and Asp[181] of hHS-2OST are marked by ☆. PAPS-binding sites are marked by *black boxes*, and the invariant cystines are marked by *gray triangles*. The percentage of amino acid identity with dmHs2st and pip-PA within the region shown is displayed in the *bottom right corner* of this figure.

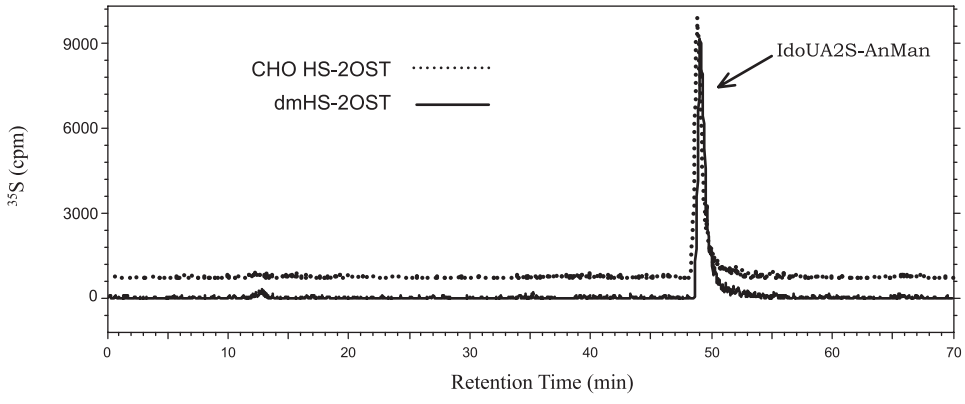

FIGURE 7. **RPIP-HPLC of the disaccharide analysis of dmHS-2OST-modified and Chinese hamster HS-2OST-modified CDSNS heparin.** CDSNS heparin were 2-*O*-^{35}S-labeled by dmHS-2OST (or by Chinese hamster HS-2OST) and [^{35}S]PAPS. The labeled heparin was subjected to low pH nitrous acid depolymerization, and the resultant ^{35}S-labeled disaccharides were resolved on RPIP-HPLC. The elution position of IdoUA2S-AnMan is indicated by an *arrow*, which is identical to the disaccharide generated from Chinese hamster (*CHO*) HS-2OST-modified CDSNS heparin.

however, additional structural features are noted. We identified four residues that potentially bind to the 5′-phosphate of PAP, and two residues that may bind to the 3′-phosphate of PAP in both enzymes (Fig. 8, *red triangle*). The Thr[84] in HS-2OST and Cys[113] in CS-2OST align with Ser[49] of hEST; however, the side chain of Ser[49] shows no direct interaction with PAPS in the crystal structure (32). Because the mutations of this position resulted in less potent activity impairment, we reasoned that T84A (or C113A) may affect the binding to PAPS indirectly by affecting the conformation of the PSB loop. In addition, we observed that HS-2OST and CS-2OST appear to utilize different residues, Thr[87] of HS-2OST *versus* Arg[116] of CS-2OST, to bind to PAPS. Our homology alignment result suggests that Thr[87] and Arg[116] align with Thr[51] in hEST as well as Arg[166] in HS 3-OST-3. Indeed, the backbone amide of Arg[166] in HS 3-OST-3 and the backbone amide as well as the hydroxyl group of Thr[51] in hEST interact with the 5′-phosphate of PAPS.

The catalytic sites of HS-2OST and CS-2OST appear to be similar to that of hEST, which uses a histidine as a catalytic base rather than a glutamate residue that has been suggested for *N*-deacetylase/*N*-sulfotransferase and the 3-OSTs (20, 27). For HS-2OST, a double mutant H140A/H142A was required to

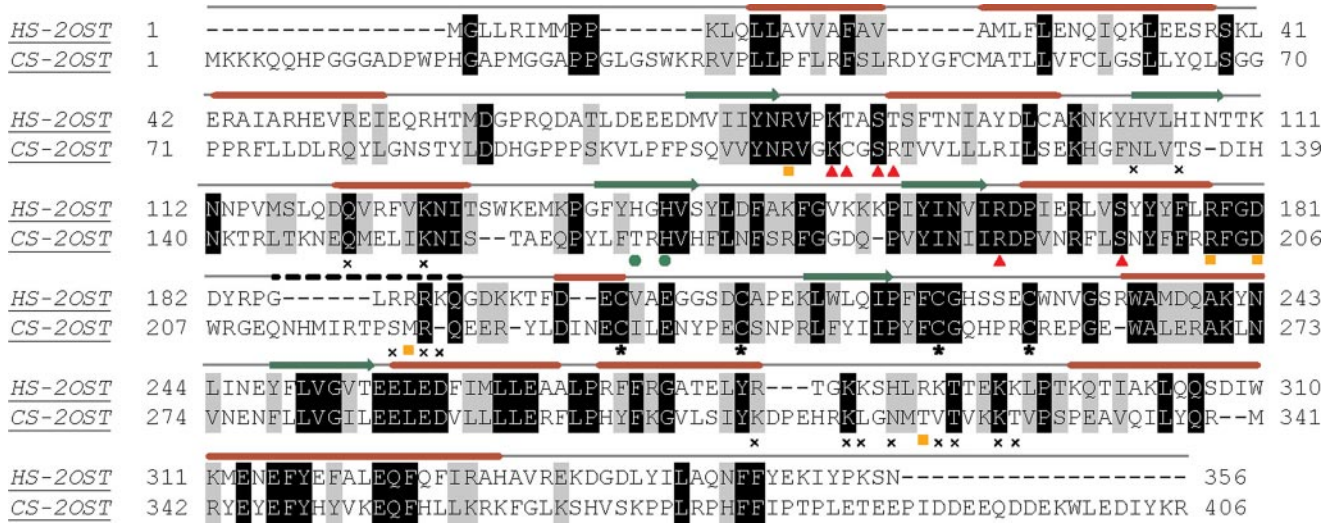

FIGURE 8. **Overview of the predicted structure of HS/CS-2OST and the examined residues.** Aligned amino acids are *boxed* and *shaded black* for identical residues and *gray* for similar residues, and the introduced *gaps* are shown as *dashes*. The predicted secondary structure (based on predictions by Gen THREADER and Predict Protein) (43) is represented on the top of the alignment as follows: α-helix in *red tube*, β-strand in *green arrow*, coil in *gray line*, and regions with very low prediction confidence as a *black dashed line*. The examined residues are marked at the bottom of the alignment as follows: PAPS-binding residues as *red triangle*, substrate-binding residues as *yellow square*, catalytic residues as *green circle*, residues with no obvious impairment on activity when mutated as ×, and the invariant cysteines as *an asterisk*.

abolish the activity, suggesting both histidine residues are important for catalysis. In contrast, the single H168A mutation was able to abolish the activity of CS-2OST. His^{142} in HS-2OST and His^{168} of CS-2OST align with the catalytic base His^{107} of hEST, which is conserved among all cytosolic STs and many Golgi STs (33), whereas His^{140} is a unique residue present only among HS-2OST. Without structural data, it is unclear about the precise roles of the two histidines in HS-2OST. One possibility is that one histidine may function as a base, and the other may help stabilize the transition state. Alternatively, both residues may be required for binding HS in a proper orientation for catalysis. Another possibility is that His^{140} and His^{142} may contribute to the catalysis in a complementary manner as has been suggested for a few other enzymes (34). In rat testis fructose-2,6-biphosphatase, His^{256} and His^{390} have been suggested to perform the catalytic function in concert. Mutations at both His^{256} and His^{390} are required to abolish the activity of fructose-2,6-biphosphatase (35). Another example of using two histidine residues in catalysis is serum paraoxonase 1 (PON1), an enzyme catalyzing the hydrolysis and formation of various lactones. His^{115} and His^{134} of PON1 form a histidine dyad in the active site and facilitate the catalysis through interactions with one another. In contrast to fructose-2,6-biphosphatase, the H115Q mutant resulted in a much more potent activity impairment (~1%) than did the H134Q mutant (~10%) with most substrates used, implicating a primary role of His^{115} and an auxiliary role of His^{134} in the catalysis of PON1 (36, 37). We hope future structural studies will shine light on the role of these histidines in catalysis.

We also explored the potential substrate-binding residues in HS-2OST and CS-2OST based on the high structural homology among the sulfotransferases. We believe that 3-*O*-sulfotransferase and 2-*O*-sulfotransferase should have very similar overall structures. Furthermore, the substrate binding domains of 3-*O*-sulfotransferase and 2-*O*-sulfotransferase should be similar. The major difference between 3-*O*-sulfotransferase and 2-*O*-sulfotransferase would be the amino acid residues in those substrate binding domains, recognizing the unique sulfo acceptor. This hypothesis has been proved by comparing the crystal structures of heparan *N*-sulfotransferase (38) and 3-*O*-sulfotranferases (20, 27). Altogether, we identified five residues in HS-2OST and four residues in CS-2OST that potentially mediate substrate binding, excluding the histidine residues involved in catalysis (Fig. 8, *yellow squares*). Mutations at four aligned residues have resulted in the loss of the activities of HS-2OST and CS-2OST, suggesting that a similar cleft exists in these enzymes as is observed for 3-OST-1, -3, and NST. The exception among the substrate-binding site mutant is D206A of CS-2OST. Mutant D206A of CS-2OST has a more potent effect on the enzymatic activity than its counterpart mutant in D181A of HS-2OST, implying a more prominent role for Asp^{206} in the substrate binding for CS-2OST.

A basic residue, Arg^{189} in HS-2OST, is of special interest. Mutant R189A has no sulfotransferase activity but maintains excellent binding affinity to PAP. We postulate that Arg^{189} participates in substrate recognition for HS-2OST based on two lines of evidence. First, this residue is located at a predicted coil section after helix 5 in HS 3-OST-3, which is quite dissimilar between HS-2OST and CS-2OST (Fig. 4). This region, including helix 5 in 3-OST-1 and HS 3-OST-3, contains numerous residues involved in substrate binding. Second, we did not find a similar basic residue in this region in CS-2OST that is essential for the sulfotransferase activity. The positively charged Arg^{189} in HS-2OST could be involved in binding to the negatively charged sulfates of HS polysaccharide substrate.

In the long coil region (Fig. 4, *blue*), we identified a position that is potentially involved in substrate binding, although utilizing different amino acid residues for HS-2OST and CS-2OST, respectively. For example, CS-2OST requires an uncharged residue, Thr^{321}, at this position, although HS-2OST

requires a positively charged residue, Arg^{288}, at this position. We postulate that Arg^{288} of HS-2OST and Thr^{321} of CS-2OST are involved in substrate recognition. It is important to note that Arg^{370} of HS 3-OST-3, the corresponding residue of Arg^{288} in HS-2OST, directly interacts with the 2-*O*-sulfo group of the iduronic acid unit at the nonreducing end of the acceptor site (27). If Arg^{288} of HS-2OST plays a similar role, this residue could directly interact with the *N*-sulfo group of the glucosamine unit at the nonreducing end of the acceptor site. In the case of CS-2OST, the Thr^{321} residue could form a hydrogen bond with the *N*-acetyl group of the GalNAc unit. It is known that HS-2OST recognizes the hexauronic acid unit that is adjacent to an *N*-sulfoglucosamine unit carrying a negative charge (15), whereas CS-2OST recognizes the hexauronic acid unit that is adjacent to *N*-acetylated galactosamine unit (Fig. 1) (31).

Those residues that are involved in substrate binding were determined based on the homology/dissimilarity to HS 3-OST-3, of which the substrate-binding sites are known. We note that there is no direct experiment to prove the mutants are defective in substrate binding because of the unavailability of the structurally defined substrates. A heterogeneous polysaccharide was used throughout this study. The complexity of this polysaccharide substrate does not allow us to distinguish between the specific substrate/enzyme interactions and nonspecific polysaccharide/protein interactions.

Finally, we demonstrated that the distribution of the amino acid residues that are essential for HS-2OST and CS-2OST can be used to identify whether a *Drosophila* protein carries 2-OST enzymatic activity. In this experiment, we found that the gene product of *Hs2st* is the *Drosophila* HS-2OST. The coexistence of equivalent residues at the His^{140} and Asp^{181} position of HS-2OST helped us recognize unambiguously that the dmHs2st is a HS-2OST, which is verified by our *in vitro* activity assay. To our knowledge, this is the first study demonstrating the substrate specificity for *Drosophila* HS-2OST, of which the roles in synthesizing the HS carrying 2-*O*-sulfated iduronic acid and regulating the embryonic development in *Drosophila* have just been explored recently (39).

Our model predicts that two gene products of the *Drosophila* gene *pipe* have no HS-2OST activity. Indeed, expression of two *pipe* gene products, pip-PA and pip-PF, was achieved. Both proteins showed neither HS nor CS sulfotransferase activities toward the substrates tested. Our result of pip-PA is consistent with a recent *in vivo* study using a *Drosophila* strain that is defective in synthesis of the backbone of HS and CS (40), suggesting the activity of pip-PA does not depend on either HS or CS. We noted that GlcUA2S or IdoUA2S units, the products of CS-2OST, are not present in CS isolated from *Drosophila* (41, 42), suggesting that pipe proteins are unlikely to carry CS-2OST activity. Considering that many CS modification enzymes, such as CS 4-*O*-sulfotransferases, share high homology to STs that sulfate the sugar moiety of glycoproteins (3), it is possible that the *pipe* genes are responsible for modifying other types of carbohydrate motifs of glycoproteins. Interestingly, HS-2OST is present and highly conserved in all sequenced bilateral animals dating back to the flatworm, whereas CS-2OST can be only identified in vertebrates, suggesting that the *CS-2OST* gene has a unique role in vertebrates.

In conclusion, we have provided a new body of information on the structural features of HS-2OST and CS-2OST through homology and extensive mutagenesis studies. This information advances our understanding of the mechanism of action of these enzymes and helps decipher how structural diversity of glycosaminoglycans is achieved.

Acknowledgment—We thank Andrea Moon for reviewing the manuscript.

Addendum—While this manuscript was under review, Kamimura *et al.* (39) reported the contributions of 2-*O*-sulfation and 6-*O*-sulfation in HS to the fibroblast growth factor signaling in *Drosophila*. In this study, the *in vivo* functions of dmHs2st were confirmed.

REFERENCES

1. Esko, J. D., and Selleck, S. B. (2002) *Annu. Rev. Biochem.* **71,** 435–471
2. Liu, J., and Thorp, S. C. (2002) *Med. Res. Rev.* **22,** 1–25
3. Kusche-Gullberg, M., and Kjellen, L. (2003) *Curr. Opin. Struct. Biol.* **13,** 605–611
4. Lindahl, U., Kusche-Gullberg, M., and Kjellen, L. (1998) *J. Biol. Chem.* **273,** 24979–24982
5. Kitagawa, H., Izumikawa, T., Uyama, T., and Sugahara, K. (2003) *J. Biol. Chem.* **278,** 23666–23671
6. Sugahara, K., Mikami, T., Uyama, T., Mizuguchi, S., Nomura, K., and Kitagawa, H. (2003) *Curr. Opin. Struct. Biol.* **13,** 612–620
7. Kreuger, J., Salmivirta, M., Sturiale, L., Gimenez-Gallego, G., and Lindahl, U. (2001) *J. Biol. Chem.* **276,** 30744–30752
8. Turnbull, J. E., Fernig, D. G., Ke, Y., Wilkinson, M. C., and Gallagher, J. T. (1992) *J. Biol. Chem.* **267,** 10337–10341
9. Bullock, S. L., Fletcher, J. M., Beddington, R. S., and Wilson, V. A. (1998) *Genes Dev.* **12,** 1894–1906
10. Bulow, H. E., and Hobert, O. (2004) *Neuron* **41,** 723–736
11. Kinnunen, T., Huang, Z., Townsend, J., Gatdula, M. M., Brown, J. R., Esko, J. D., and Turnbull, J. E. (2005) *Proc. Natl. Acad. Sci. U. S. A.* **102,** 1507–1512
12. Maimone, M. M., and Tollefsen, D. M. (1990) *J. Biol. Chem.* **265,** 18263–18271
13. Bao, X., Pavão, M. S. G., dos Santos, J. C., and Sugahara, K. (2005) *J. Biol. Chem.* **280,** 23184–23193
14. Hikino, M., Mikami, T., Faissner, A., Vilela-Silva, A., Pavão, M. S. G., and Sugahara, K. (2003) *J. Biol. Chem.* **278,** 43744–43754
15. Rong, J., Habuchi, H., Kimata, K., Lindahl, U., and Kusche-Gullberg, M. (2001) *Biochemistry* **40,** 5548–5555
16. Kobayashi, M., Sugumaran, G., Liu, J., Shworak, N. W., Silbert, J. E., and Rosenberg, R. D. (1999) *J. Biol. Chem.* **274,** 10474–10480
17. Ohtake, S., Kimata, K., and Habuchi, O. (2005) *J. Biol. Chem.* **280,** 39115–39123
18. Sen, J., Goltz, J. S., Stevens, L., and Stein, D. (1998) *Cell* **95,** 471–481
19. Zheng, L., Baumann, U., and Reymond, J. (2004) *Nucleic Acids Res.* **32,** e115
20. Edavettal, S. C., Lee, K. A., Negishi, M., Linhardt, R. J., Liu, J., and Pedersen, L. C. (2004) *J. Biol. Chem.* **279,** 25789–25797
21. Chen, J., Avci, F. Y., Muñoz, E. M., McDowell, L. M., Chen, M., Pedersen, L. C., Zhang, L., Linhardt, R. J., and Liu, J. (2005) *J. Biol. Chem.* **280,** 42817–42825
22. Shively, J. E., and Conrad, H. E. (1976) *Biochemistry* **15,** 3932–3942
23. Shworak, N. W., Shirakawa, M., Colliec-Jouault, S., Liu, J., Mulligan, R. C., Birinyi, L. K., and Rosenberg, R. D. (1994) *J. Biol. Chem.* **269,** 24941–24952
24. Negishi, M., Pedersen, L. G., Petrotchenko, E., Shevtsov, S., Gorokhov, A., Kakuta, Y., and Pedersen, L. C. (2001) *Arch. Biochem. Biophys.* **390,** 149–157
25. McGuffin, L. J., and Jones, D. T. (2003) *Bioinformatics* (*Oxf.*) **19,** 874–881
26. Kakuta, Y., Petrotchenko, E. V., Pedersen, L. C., and Negishi, M. (1998) *J. Biol. Chem.* **273,** 27325–27330

27. Moon, A., Edavettal, S. C., Krahn, J. X., Munoz, E. M., Negishi, M., Linhardt, R. J., Liu, J., and Pedersen, L. C. (2004) *J. Biol. Chem.* **279,** 45185–45193
28. Sergeev, P., Streit, A., Heller, A., and Steinmann-Zwicky, M. (2001) *Dev. Dyn.* **220,** 122–132
29. Sen, J., Goltz, J. S., Konsolaki, M., Schupbach, T., and Stein, D. (2000) *Development* (*Camb.*) **127,** 5541–5550
30. Pinhal, M. A., Smith, B., Olson, S., Aikawa, J., Kimata, K., and Esko, J. D. (2001) *Proc. Natl. Acad. Sci. U. S. A.* **98,** 12984–12989
31. Kobayashi, M., Habuchi, H., Yoneda, M., Habuchi, O., and Kimata, K. (1997) *J. Biol. Chem.* **272,** 13980–13985
32. Pedersen, L. C., Petrotchenko, E., Shevtsov, S., and Negishi, M. (2002) *J. Biol. Chem.* **277,** 17928–17932
33. Kakuta, Y., Pedersen, L. G., Carter, C. W., Negishi, M., and Pedersen, L. C. (1997) *Nat. Struct. Biol.* **4,** 904–908
34. Gutteridge, A., and Thornton, J. M. (2005) *Trends Biochem. Sci.* **30,** 622–629
35. Mizuguchi, H., Cook, P. F., Tai, C. H., Hasemann, C. A., and Uyeda, K. (1999) *J. Biol. Chem.* **274,** 2166–2175
36. Harel, M., Aharoni, A., Gaidukov, L., Brumshtein, B., Khersonsky, O., Meged, R., Dvir, H., Ravelli, R. B. G., McCarthy, A., and Toker, L. (2004) *Nat. Struct. Biol.* **11,** 412–419
37. Khersonsky, O., and Tawfik, D. S. (2006) *J. Biol. Chem.* **281,** 7649–7656
38. Kakuta, Y., Sueyoshi, T., Negishi, M., and Pedersen, L. C. (1999) *J. Biol. Chem.* **274,** 10673–10676
39. Kamimura, K., Koyama, T., Habuchi, H., Ueda, R., Masayuki, M., Kimata, K., and Nakato, H. (2006) *J. Cell Biol.* **174,** 773–778
40. Zhu, X., Sen, J., Stevens, L., Goltz, J. S., and Stein, D. (2005) *Development* (*Camb.*) **132,** 3813–3822
41. Toyoda, H., Kinoshita-Toyoda, A., and Selleck, S. B. (2000) *J. Biol. Chem.* **275,** 2269–2275
42. Pinto, D. O., Ferreira, P. L., Andrade, L. R., Petrs-Silva, H., Linden, R., Abdelhay, E., Araujo, H. M. M., Alonso, C. E. V., and Pavao, M. S. G. (2004) *Glycobiology* **14,** 529–536
43. McGuffin, L. J., Bryson, K., and Jones, D. T. (2000) *Bioinformatics* (*Oxf.*) **16,** 404–405